REVISTA INTERDISCIPLINAR DE PESQUISA EM ENGENHARIA

CILAMCE 2016

XXXVII IBERIAN LATIN AMERICAN CONGRESS ON COMPUTATIONAL METHODS IN ENGINEERING
BRASÍLIA - DF - BRAZIL

A FRETTING PROBLEM ANALYSIS USING THE BOUNDARY ELEMENT METHOD

Bruno Cavalcante

Eder Lima de Albuquerque

Thiago Doca

bruno.melocavalcante@gmail.com

eder@unb.br

doca@unb.br

University of Braslia

Asa Norte, 70910-900, Braslia, DF, Brazil

Mohammad Hossein Shaterzadeh-Yazdi

Paulo Sollero

mohammad@fem.unicamp.br

sollero@fem.unicamp.br

University of Campinas

Rua Mendeleyev, 200, 13083-860, Campinas, SP, Brazil

Abstract. *Fretting occurs whenever the interface between components is subjected to a variable load, since it creates a finite relative tangential displacement over at least part of the contact zone. This phenomena has been the focus of many researches for being one of the main causes of mechanical failure. Additionally, fretting has been recognized as one of the costliest sources of in-service damage relate to high cycle fatigue (HCF) in many applications.*

Keywords: *Contact Mechanics, The Boundary Element Method, Fretting, Newton Method)*

1 INTRODUCTION

In his famous paper on the contact of elastic bodies in 1881 (Hertz, 1881), Heinrich Hertz increased the attention on contact mechanics by mixing classic mechanic laws and the elasticity theory. Although restricted a few problems, the content of his work brought interest to the field and enhanced the technological importance of contact mechanics in engineering.

He investigated contact of elastic bodies under certain restrictions and derived the pressure distribution in the contact area. This concepts are essential to the resolution of contact problems. The unfamiliarity with the value of the contact area features the non-linearity of the contact problems. The contact pressure peaks from zero to the maximum pressure when enters the contact area, characterizing a high gradient problem.

Finite Element Method (FEM) helped to increase the number of contact problems that can be solved. During the sixties the first codes like HEMP-hydrocode could deal with small contact problems and later in the seventies, explicit programs like DYNA2D and DYNA3D and implicit programs such as NIKE2D and NIKE3D provided the possibility to solve large scale contact problems in a efficient way (Wriggers, 2006).

However, Finite Element's necessity to discretise the entire domain proved to be computationally expensive, especially when solving large problems. In order to fix this, mesh reduction methods are being develop. The study of the phenomenon and modelling of contact problems, using the Boundary Element Method (BEM), are presented in this work. According to Popov (2010), BEM is especially suited for calculating contacts, because only the discretisation of the surface is necessary.

BEM has a series of advantages over other numerical techniques. It reduces the dimensionality of the problem by one, resulting in a smaller system of equations, offers continuous modelling within the solution domains, in other words, the lack of domain discretisation leads to a higher resolution of interior stresses and displacements. Different than traditional Finite Element formulation, in BEM displacements and tractions are calculated with the same accuracy. Lastly, the method is well suited to problems of infinite and semi-infinite domains, such as soil mechanics and acoustics (Wrobel, 2002), and for high gradient problems like wave propagation, crack propagation and contact mechanics.

The developed formulation is employed for the analysis of the Cattaneo-Mindlin problem where two cylindrical pads are initially submitted to a vertical monotonic load followed by a horizontal cyclic load. This problem covers the mixed contact behaviour of fretting as proposed initially by Eden et al. (1911) and Tomlison (1927). Furthermore, as it has an analytical solution, it is well suited to assess numerical methods. The analysis is conducted with the use of quadratic continuous elements which provides non-oscillatory results.

2 BOUNDARY ELEMENT METHOD IN ELASTICITY

The BEM formulation in elasticity can be found in many classical texts (Brebbia, 1996; Aliabadi, 2002). The equilibrium equation is transformed in a boundary integral equation using Betti's theorem. This equation is given by,

$$C_{ij}(x)u_j(x) + \int_\Gamma T_{ij}(x,x')u_j(x')d\Gamma = \int_\Gamma U_{ij}(x,x')t_j(x')d\Gamma, \tag{1}$$

where u and t are, respectively, the displacement vector and the boundary tractions. The coefficient C_{ij} is geometry dependent, $\frac{1}{2}$ for smooth boundaries. Lastly, $U_{ij}(x, x')$ and $T_{ij}(x, x')$ are the fundamental solutions for displacements and tractions. They represent the response of the field point x' when a traction or a displacement is applied in the source point x. Expressions for the fundamental solution can be found in traditional literature (Aliabadi, 2002).

Dividing the boundary Γ in N_e elements the integral Eq. (1) can be rewritten as:

$$C_{ij}u_j + \sum_{j=1}^{Ne} \int_{\Gamma_j} T^*_{ik} u_i d\Gamma_j = \sum_{j=1}^{Ne} \int_{\Gamma_j} U^*_{ik} t_j d\Gamma_j \tag{2}$$

Basically, Eq. (2) evaluates the value of the fundamental solutions when one node turns into the source point. This process is done to all nodes forming a linear system, that can be simplified as:

$$\mathbf{Hu} = \mathbf{Gt}, \tag{3}$$

such that $\int_{\Gamma_j} \mathbf{UN} d\Gamma = \mathbf{G}$ and $\int_{\Gamma_j} \mathbf{TN} d\Gamma = \mathbf{H}$

Matrices **H** and **G** contain the fundamental solutions (tractions and displacements), and the vectors **u** and **t** contain the nodal displacements and tractions. Applying the boundary conditions in Eq. (3) the system is simplified to:

$$\mathbf{Ax} = \mathbf{b}, \tag{4}$$

where matrix **A** contains a mix of columns of matrices **H** and **G**, **x** is the vector of unknowns, and vector **b** stands for the product of the remainder columns of matrices **H** and **G** by the value of boundary conditions.

3 CONTACT FORMULATION

The contact formulation employed here is derived from the Theory of Elasticity. First, two bodies in contact are considered enclosed by their respective boundaries setting two defined domains, the contact domain Γ_c and the non-contact domain Γ_{nc}, as depicted in Fig. 1.

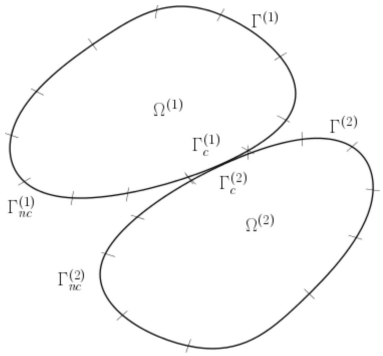

Figure 1: Two bodies in contact

When two bodies are in contact due to a external loading, the boundary integral equation is applied on each body in order to describe their respective displacements and tractions, such as:

$$C_{ij}^1 u_j^1 + \int_{\Gamma_{nc}^1} T_{ij}^1 u_j^1 d\Gamma^1 + \int_{\Gamma_c^1} T_{ij}^1 u_j^1 d\Gamma^1 = \int_{\Gamma_{nc}^1} U_{ij}^1 t_j^1 d\Gamma^1 + \int_{\Gamma_c^1} U_{ij}^1 t_j^1 d\Gamma^1 \tag{5}$$

$$C_{ij}^2 u_j^2 + \int_{\Gamma_{nc}^2} T_{ij}^2 u_j^2 d\Gamma^2 + \int_{\Gamma_c^2} T_{ij}^2 u_j^2 d\Gamma^2 = \int_{\Gamma_{nc}^2} U_{ij}^2 t_j^2 d\Gamma^2 + \int_{\Gamma_c^2} U_{ij}^2 t_j^2 d\Gamma^2 \tag{6}$$

Equations (5) and (6) can be taken to the discrete domain just as in equation (2):

$$c_{ij}^1 u_j^1 + \sum_{n=1}^{N} H_{ij}^{n^1} u_j^{n^1} = \sum_{n=1}^{N} G_{ij}^{n^1} t_j^{n^1} \tag{7}$$

$$c_{ij}^2 u_j^2 + \sum_{m=1}^{M} H_{ij}^{m^B} u_j^{m^2} = \sum_{m=1}^{M} G_{ij}^{m^2} t_j^{m^2} \tag{8}$$

where m and n are the total number of nodes in body 1 and 2, respectively. This group of linear system is represented by:

$$\mathbf{H^1 u^1 = G^1 t^1} \quad \textbf{and} \quad \mathbf{H^2 u^2 = G^2 t^2} \tag{9}$$

The linear systems are later coupled because they share nodes in the contact zone Γ_c. However, at this point, the contact zone is unknown. This requires an interactive solution scheme that requires the consideration of a possible contact zone. The other region Γ_{nc} is contained in a mixed matrix, $A_{nc}^{1,2}$, which does not change during the solution process,

$$\begin{bmatrix} \mathbf{A}_{nc}^1 & 0 & \mathbf{H}_c^1 & 0 & \textbf{-}\mathbf{G}_c^1 & 0 \\ 0 & \mathbf{A}_{nc}^2 & 0 & \mathbf{H}_c^2 & 0 & \textbf{-}\mathbf{G}_c^2 \\ 0 & 0 & \mathbf{C}_u^1 & \mathbf{C}_u^2 & \mathbf{C}_t^1 & \mathbf{C}_t^2 \end{bmatrix} \begin{Bmatrix} \mathbf{x}_{nc}^1 \\ \mathbf{x}_{nc}^2 \\ \mathbf{u}_c^1 \\ \mathbf{u}_c^2 \\ \mathbf{t}_c^1 \\ \mathbf{t}_c^2 \end{Bmatrix} = \begin{Bmatrix} \mathbf{b}^1 \\ \mathbf{b}^2 \\ \mathbf{v}^{1,2} \end{Bmatrix} \tag{10}$$

Furthermore, the traction and displacements are also unknowns of the problem, resulting in a system with more variables than equations. In order to fulfil this condition, constraints relating the displacements $c_u^{1,2}$ and the tractions $c_t^{1,2}$ are created. These constraints are allocated in the contact vector $v^{1,2}$, which is added to the right side of the Eq. (10) in order to account for the gap between the bodies.

The constraints depend on which contact mode their respective nodes are: slip, stick or non-contact condition:

Slip:

$$\mathbf{c}_u = \begin{bmatrix} 0 & 0 & 0 & 0 \\ 0 & 0 & 0 & 0 \\ 1 & 0 & 1 & 0 \\ 0 & 0 & 0 & 0 \end{bmatrix} \qquad \mathbf{c}_t = \begin{bmatrix} 1 & 0 & -1 & 0 \\ \pm\mu & 1 & 0 & 0 \\ 0 & 0 & 0 & 0 \\ 0 & 0 & \pm\mu & 1 \end{bmatrix}$$

Stick:

$$\mathbf{c}_u = \begin{bmatrix} 0 & 0 & 0 & 0 \\ 0 & 0 & 0 & 0 \\ 1 & 0 & 1 & 0 \\ 0 & 1 & 0 & 1 \end{bmatrix} \qquad \mathbf{c}_t = \begin{bmatrix} 1 & 0 & -1 & 0 \\ 0 & 1 & 0 & -1 \\ 0 & 0 & 0 & 0 \\ 0 & 0 & 0 & 0 \end{bmatrix}$$

Non-contact:

$$\mathbf{c}_u = \begin{bmatrix} 0 & 0 & 0 & 0 \\ 0 & 0 & 0 & 0 \\ 0 & 0 & 0 & 0 \\ 0 & 0 & 0 & 0 \end{bmatrix} \qquad \mathbf{c}_t = \begin{bmatrix} 1 & 0 & 0 & 0 \\ 0 & 1 & 0 & 0 \\ 0 & 0 & 1 & 0 \\ 0 & 0 & 0 & 1 \end{bmatrix}$$

The solution of the equation system can be performed using a residual function (Rodríguez-Tembleque et al., 2010, 2011),

$$\mathbf{R} = \mathbf{A}\mathbf{x} - \mathbf{b}, \tag{11}$$

where the matrix **A** contains all the coefficients from (10) located in the left side of the equation, **x** the variables and the vector **b**, the group in the right side of the equation. to solve equation (11) it is necessary to find a vector **x** that results in $||\mathbf{R}|| \cong 0$. Here, the method used to fulfill 11 is the Newton's method (Hoffman and Frankel, 2001).

4 NUMERICAL MODELLING

4.1 Incremental loading

In contact problems, the final solution is only obtained when the maximum loading or contact region is achieved. However, the as the possible contact zone is a function of the applied load and the coefficient of friction, the solution must be obtained with the assistance of an interactive numerical solution. If the boundaries are non-conforming ones, the result is obtained with the gradual application of the boundary condition in a series of steps.

The numerical modeling of contact problems usually requires two main schemes in its framework: incremental loading and contact evaluation.

Incremental loading leads to precise results while recording the history of the contact tensions, which is important in fretting analysis (Man, 1994).

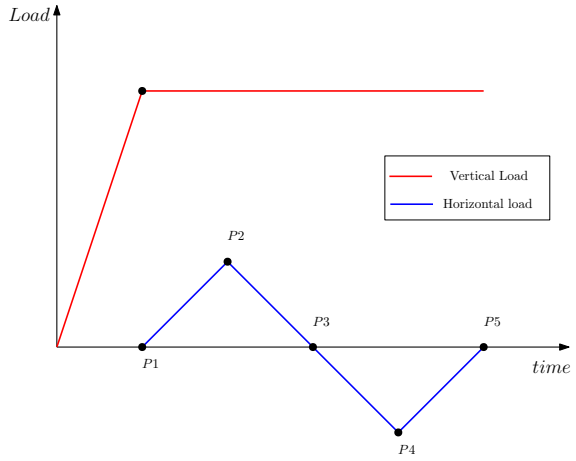

Figure 2: Incremental loading scheme

4.2 Contact detection

It is important to remember that the constraints must be satisfied and with the formulation presented in Eq. (10) they can vary on each step of the increment. Therefore, the contact regions are verified in every step but the linear part is not changed, only the constraints matrices. This means that as the possible contact zone is smaller, the solution of the system is easier to find. In order to evaluate the Cattaneo-Mindlin problem, 5 loading phases must be applied: the first one is the normal force, the second and fifth are a tangential loads to the right-side while the third and fourth are tangential loads to the left-side. This represents a full fretting cycle as denoted in figure 2, where P_n are the moments of force application.

As previously mentioned, the contact mode is verified on each incremental step in order to decide which nodes are in contact and which are not. Considering any two nodes a and b that are separated in the step $m-1$ continue to be so if in step m:

$$(\Delta u_n^a + \Delta u_n^b)^m < g_0^{m-1}$$

and

$$t_n^{m-1} + \Delta t_n^m \geq 0 \tag{12}$$

And are in contact if:

$$(\Delta u_n^a + \Delta u_n^b)^m \geq g_0^{m-1} \tag{13}$$

and

$$t_n^{m-1} + \Delta t_n^m < 0 \tag{14}$$

g_0 being the gap between the bodies and u_n and t_n the normal displacement and normal traction. Another decision must be made, since in fretting the nodes are in partial slip conditions, so there must be a way to determine if the nodes are in stick or slip.

In this case, is enough to test the stick state as follows,

$$|t_t^m| = |t_t^{m-1} + \Delta t_t^m| \leq \mu |t_n^{m-1} + \Delta t_n^m| = \mu \, |t_n^m| \tag{15}$$

If this conditions are valid, the contact domains remain in a stick state. Else:

$$|t_t^{m-1} + \Delta t_t^m| \geq \mu |t_n^{m-1} + \Delta t_n^m| \tag{16}$$

the bodies slip condition is achieved.

The Coulomb's law of friction, defines two friction coefficients, a static and a dynamic one. However, in problems where there are both slip and stick simultaneously present, μ can be approximated to an average value (Nowell and Hills, 1987). This simplification is made here.

5 RESULTS

5.1 Mesh and boundary conditions

The numerical example consists in two cylindrical surfaces in contact due to a normal applied force followed by a series of vertical forces to emulate fretting behaviour. The geometry applied and the material properties are presented in table 1:

Table 1: Geometric and material properties

Properties	Symbol	Value
$Radius$	R	$70\ mm$
$Width$	w	$6.5\ mm$
$Height$	h	$6.5\ mm$
$Elasticity\ modulus$	E	$73.4\ GPa$
$Poisson's\ ratio$	ν	0.33
$Vertical\ force$	P	$100\ N/mm$
$Horizontal\ force$	Q	$15\ N/mm$

The boundary element algorithm used quadratic continuous elements to reach a better convergence ratting. In the case of figure 3, 60 quadratic continuous elements are used in each contact interface (circumference arcs). In total, each body contains 162 boundary elements (324 nodes, 648 degrees of freedom) and to colour the domain, 584 internal points were used.

5.2 Convergence Study

To assess the code's accuracy, an error analysis was carried out by evaluating the sizes of the contact zone (a) and of the stick zone (c). Analytical solutions for both variables are widely disclosed Johnson (1987), contact half width and the stick zone size formulas are:

$$a^2 = \frac{2PR}{\pi E^*} \tag{17}$$

$$\frac{c}{a} = \sqrt{a - |Q/\mu P|} \tag{18}$$

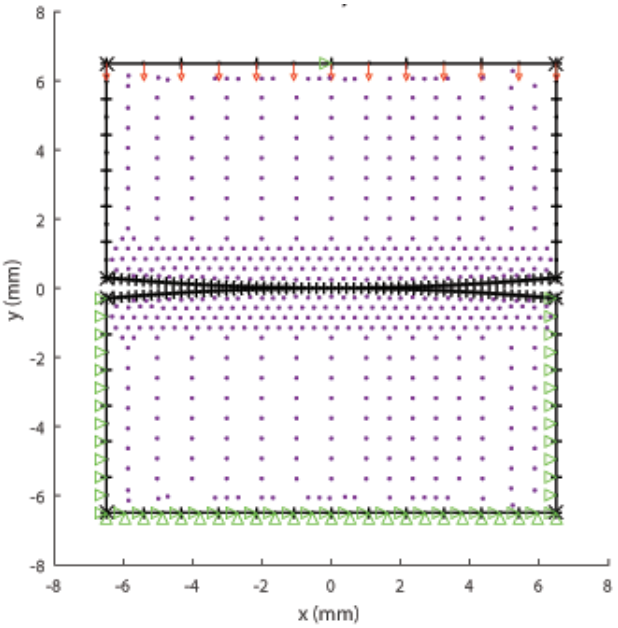

Figure 3: Boundary element mesh of the problem

E^* combines the elastic moduli and the Poisson's ratios of each body $\frac{1}{E^*} = \frac{1-v_1^2}{E_1} + \frac{1-v_2^2}{E_2}$, R is the effective radius between two spherical bodies, $\frac{1}{R} = \frac{1}{R_1} + \frac{1}{R_2}$.

To acquire numerical results, each contact node was evaluated for separation, stick or slip, and its respective coordinates were used to compute a and e.

Figure 4 exhibits the percentage error for the contact area in function of the number of elements used on the contact interface. The numerical results were obtained by simulating the problem until point P1 (figure 2), where only the vertical load was applied, and increasing the number of contact elements.

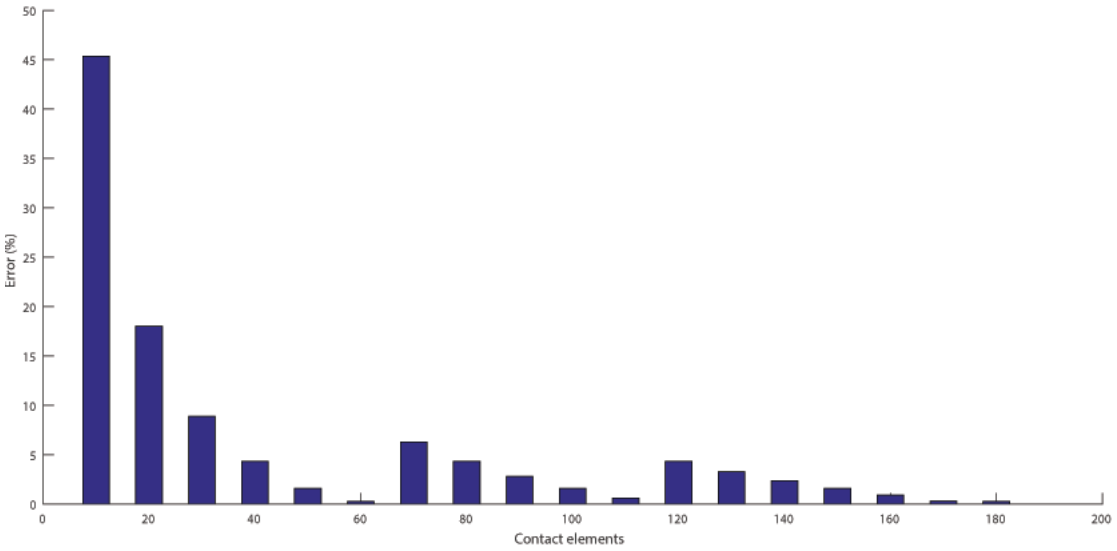

Figure 4: Evolution of the contact area relative error at P1

It can be seen that the error reduces as the elements increase until the value of 60 contact

elements is reached. Later, the error presents cyclic peaks that become smaller when more elements are used. This happens because this type of problem is called of high gradient, meaning that it possess rapid variations in its results. Therefore, they rely on node positioning and if their accumulation in the contact interface changes, it leads to a variation in the contact decision that changes the numerical value of a. This behaviour can be traced to the used mesh generator, it uses a reference value to split the geometric segment uniformly. The ideal is to use an adaptive mesh generator and its ability to places the new nodes in the high variation zones.

Figure 5 presents a bar graphic with the percentage error for the stick zone size. The results were taken in the same manner as for the contact area, except that these answers were taken in P2 (2), with the tangential force present.

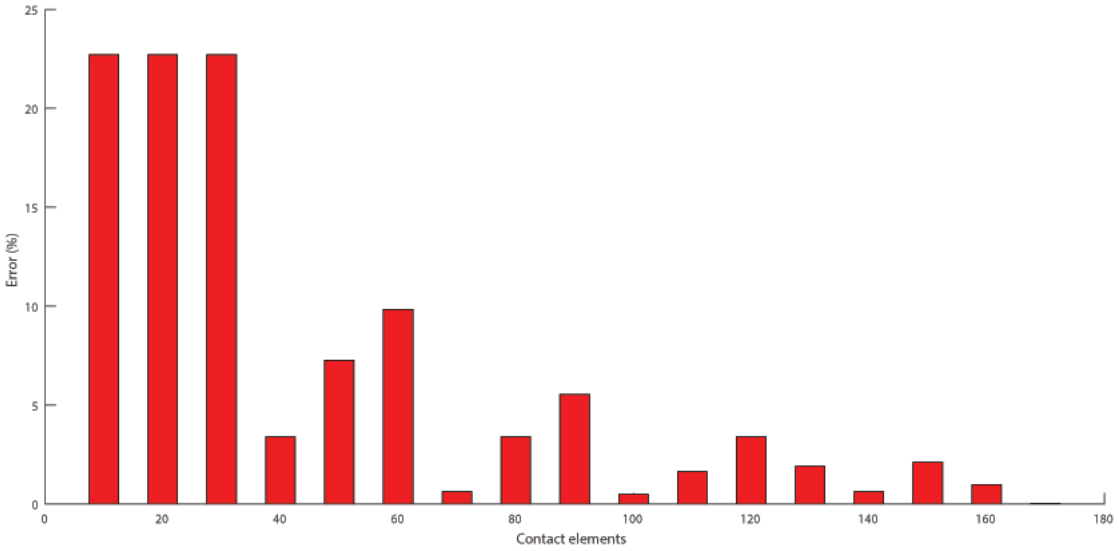

Figure 5: Evolution of the stick zone relative error at P2

High gradient behaviour of errors is more clear in this case, as the first three results presented equal solutions for the error. The stick nodes stayed grouped until 40 contact elements were used. The cyclic behaviour of errors can also be observed as in figure 4, in the end dropping to near zero values.

5.3 Problem Analysis

Figures 6, 7, 8, 9, 10 show the numerical contact pressure calculated and compared on each phase of the simulation (P1-P5) , ally to the analytical solution for partial slip found in the literature (Hills and Nowell, 1994). The results with 130 quadratic contact elements show good agreement with the analytical solution in every step of the cycle. Figure 6, the pure normal tension highlights the formation of the contact zone which remains invariable trough the whole simulation. In figure 7, it is possible to observe the mixed regime of partial slip, with the formation of a adhesion zone. Figure 8 shows the residual stresses when the tangential force returns the system to its initial configuration. Lastly, figures 9 and 10 show that the application of a inverted force. The behaviour remains the same as in P2 and P3. In these figures, it can be seen an excellent agreement of numerical and experimental results. No oscillation is presented and all peaks are accurately obtained.

Figure 11 display the color maps of the domain, painted with the von Mises criteria from P1 to P5. Results at internal points in BEM are computed by boundary integral equation using displacements and tractions solutions obtained in the boundary. So, internal points, in elastic cases, are not necessary for the problem's resolution, they are only computed only to build color maps for von Mises equivalent stresses.

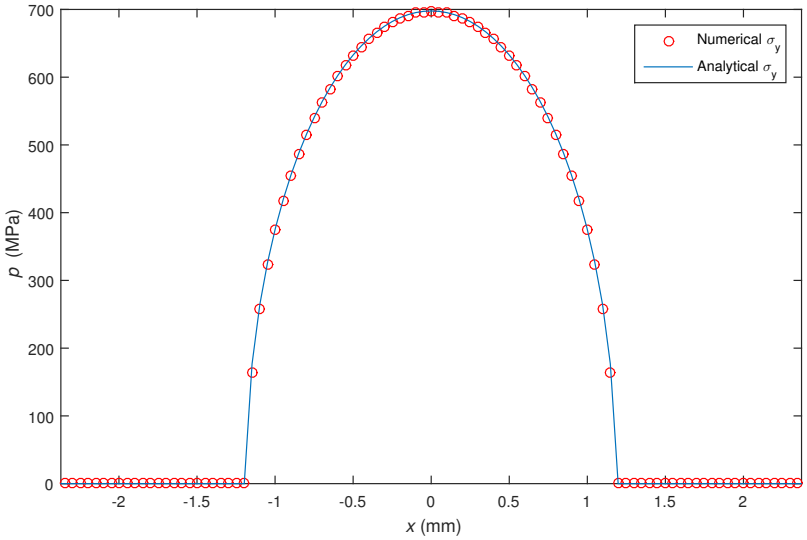

Figure 6: Contact pressure in P1

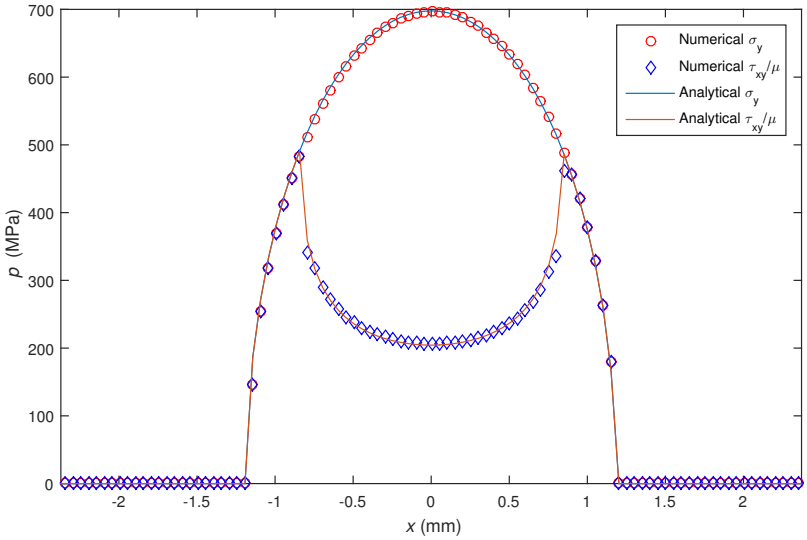

Figure 7: Contact pressure in P2

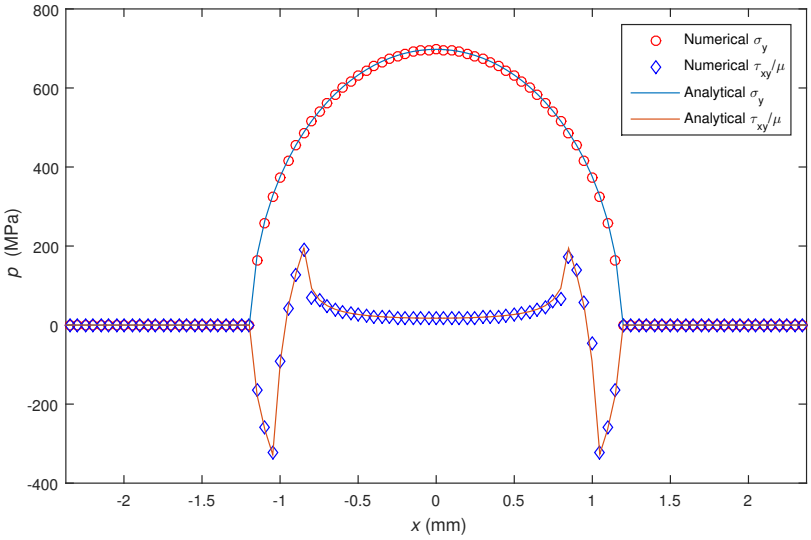

Figure 8: Contact pressure in P3

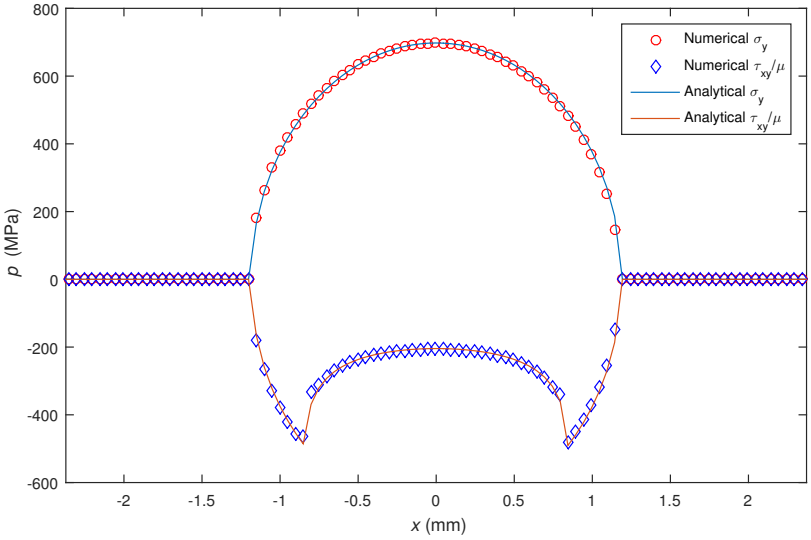

Figure 9: Contact pressure in P4

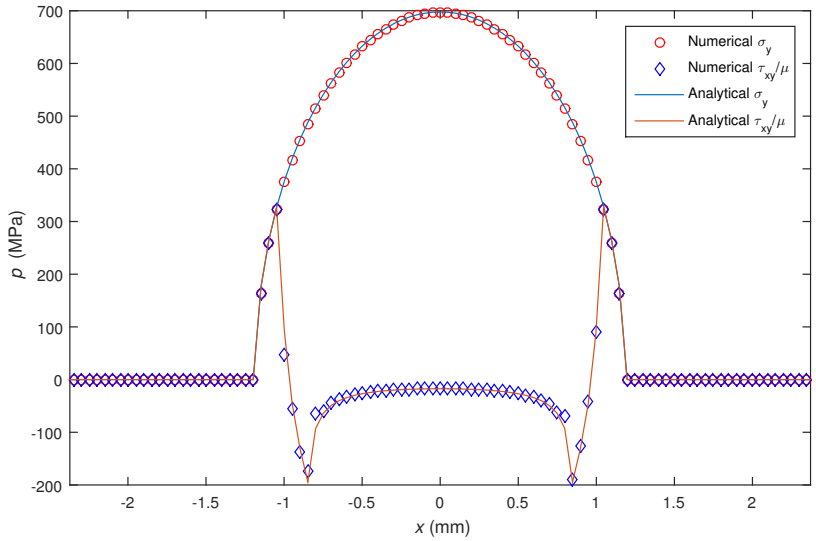

Figure 10: Contact pressure in P5

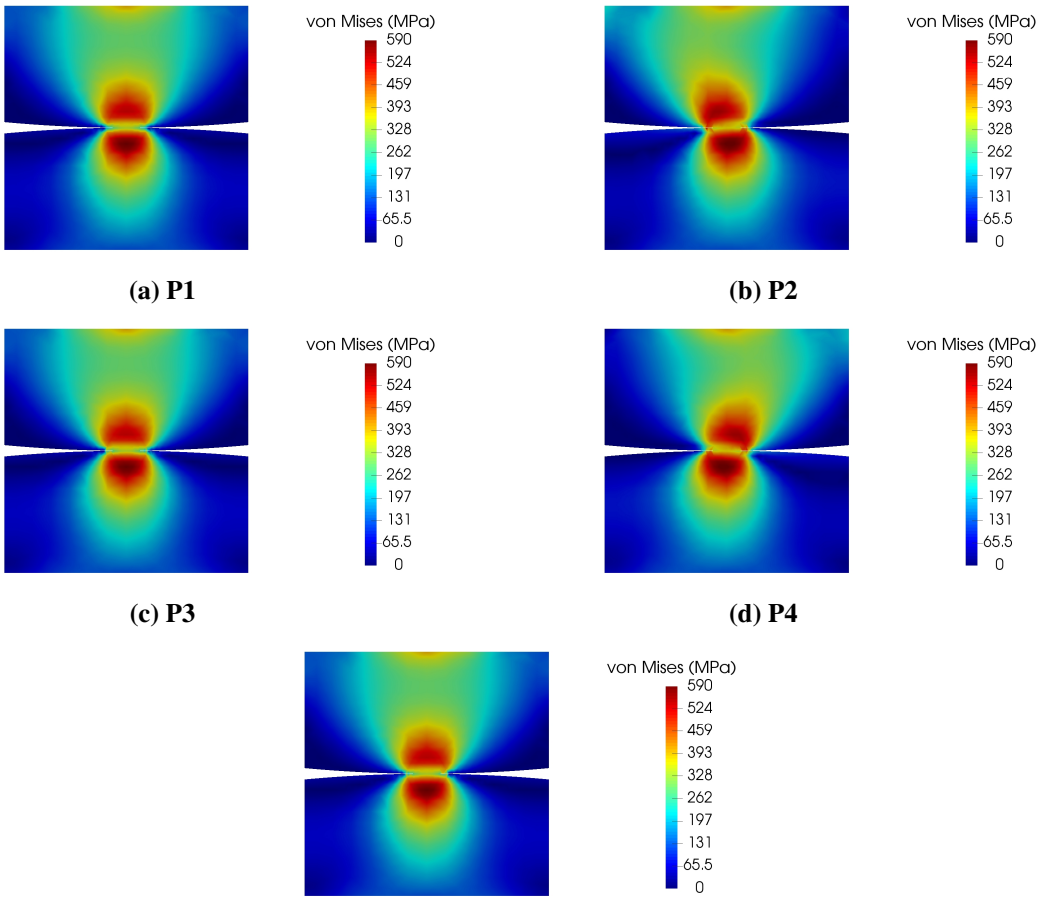

(a) P1

(b) P2

(c) P3

(d) P4

(e) P5

Figure 11: Colour maps of the von Mises Stress distribution

6 CONCLUSIONS

This article presented an analysis of the Cattaneo-Mindlin problem with a quadratic continuous boundary element formulation. Displacements and tractions are computed very accurately in the contact zone with a reduced number of degrees of freedom. Each body were modelled separately and contact conditions were imposed in the contact zone. As the contact regions is unknown in advance, the system of equations become an unconstrained non-linear problem. Newton method was used in order to compute the unknowns.

The advantages of this formulation over traditional finite element approach are the reduced number of degrees of freedom an the fact that non-linear problem is unconstrained. In finite elements, as only displacements are variables of the problem, it is necessary to use penalty or Lagrange multipliers in order to introduce tractions in the unknowns. Also, the use of quadratic or higher order elements is straight forward. In finite elements due to constrained equations, the extensions from linear to higher order elements demands a lot of work.

All results were compared with the analytical solutions and presented good agreement in all cases without oscillation and with a very good detection of peaks.

ACKNOWLEDGEMENTS

The authors would like to acknowledge the Capes/Brazil for the scholarship offered to B. Cavalcante.

REFERENCES

Aliabadi, M. H. *The Boundary Element Method, Applications in Solids and Structures*. John Wiley & Sons, 2002.

Brebbia, C. *Boundary Elements: An Introductory Course*. WIT Press, 1996.

Eden, E. M., Rose, W. N., and Cunningham, F. L. The endurance of metals: experiments on rotating beams at University College, London. *Proc. Inst. Mech. Eng.*, 4:839–974, 1911.

Hertz, H. Über die Berührung fester elastischer Körper. *J. für die reine und Angew. Math.*, 171: 156–171, 1881.

Hills, D. A. and Nowell, D. *Mechanics of Fretting Fatique*, volume 30 of *Solid Mechanics and Its Applications*. Springer Netherlands, Dordrecht, 1994.

Hoffman, J. D. and Frankel, S. *Numerical Methods for Engineers and Scientists, Second Edition*. CRC Press, second edition, 2001.

Johnson, K. L. *Contact Mechanics*. Cambridge University Press, 1987.

Man, K. W. *Contact mechanics using boundary elements*. Computational Mechanics Publications, 1994.

Nowell, D. and Hills, D. A. Mechanics of fretting fatigue tests. *Int. J. Mech. Sci.*, 29(5): 355–365, 1987.

Popov, V. L. Contact Mechanics and Friction. *Contact Mech. Frict.*, pages 55–70, 2010.

Rodríguez-Tembleque, L., Abascal, R., and Aliabadi, M.H. A boundary element formulation for wear modeling on 3D contact and rolling-contact problems. *Int. J. Solids Struct.*, 47 (18-19):2600–2612, sep 2010.

Rodríguez-Tembleque, L., Abascal, R., and Aliabadi, M.H. A boundary elements formulation for 3D fretting-wear problems. *Eng. Anal. Bound. Elem.*, 35(7):935–943, jul 2011.

Tomlison, G. A. The Rusting of Steel Surfaces in Contact . *Proc. R. Soc. London. Ser. A, Contain. Pap. a Math. Phys. Character.*, 115(771):472–483, 1927.

Wriggers, P. *Computational contact mechanics*. Springer, 2006.

Wrobel, L. C. *The Boundary Element Method, Applications in Thermo-Fluids and Acoustics*. John Wiley & Sons, 2002.